Measurement 41 (2008) 1077–1092

Contents lists available at ScienceDirect

Measurement

journal homepage: www.elsevier.com/locate/measurement

Yarn hairiness and diameter characterization using a CMOS line array

Vítor Carvalho [a,*], Michael Belsley [b,1], Rosa M. Vasconcelos [c,2], Filomena O. Soares [a,3]

[a] DEI, UM, Azurém, Guimarães, Portugal
[b] DF, UM, Gualtar, Braga, Portugal
[c] DET, UM, Azurém, Guimarães, Portugal

ARTICLE INFO

Article history:
Received 4 September 2007
Received in revised form 27 February 2008
Accepted 27 February 2008
Available online 14 March 2008

Keywords:
Yarn hairiness and diameter
Line array CMOS optical sensors
Signal processing
Electronic instrumentation

ABSTRACT

This paper presents a new system for determining yarn hairiness and diameter using a CMOS linear array together with a data acquisition board and custom developed software. The final image is generated using coherent optical signal processing with a Fourier high-pass spatial filter. The system was previously tested and validated in simulation using an image analysis line profile tool. Several analyses were performed in a laboratorial environment testing different yarns.

Finally, the results obtained with this new system are compared to those obtained previously using a simple photodiode in place of the linear photodiode array. The new system is more precise although the data processing requires significant computational effort.

1. Introduction

For yarn producers, it is very important to determine yarn hairiness, as well as yarn diameter and possible irregularities. In our previous studies [1–6], two systems were developed, based on the coherent optical signal processing techniques using a single photodiode. One system quantifies the degree of yarn hairiness while the other system was designed to characterize yarn faults based on the average diameter. This paper describes a new system for complete yarn characterization that combines these two functions, using a single linear photodiode array.

1.1. Optical and electronic hardware

In order to measure yarn hairiness and diameter, the new system includes an optical and an electronic setup. Fig. 1 presents the optical hardware [1–6].

The objective of the optical setup is to produce an image that can be analysed to provide information regarding the local degree of yarn hairiness and yarn core diameter in the final image plane (position of the photo detector shown in Fig. 1) (I/PD). Coherent light from the laser diode in a single transverse mode is incident on a beam expander lens (L1) and is directed to the yarn, placed in the object holder (O). The size of the object image is controlled by lenses L2 and L3.

A custom spatial filter (F) is placed in the Fourier plane of L2, to process the image, permitting only the high spatial frequencies in the image to propagate further (high-pass spatial Fourier filter) [7–10]. This results in the contours of the edges of the yarn and associated hairs being highlighted while simultaneously eliminating the constant background (Fig. 2).

Fig. 3 presents the block diagram of the developed electronic instrumentation hardware.

The objective of the electronic hardware is to obtain a voltage proportional to the brightness of the final image [3]. The output of a trans-impedance amplifier [11] connected to the photodiode is read by a data acquisition board (DAQ) from National Instruments [12]. LabVIEW based software was developed for acquisition control and data processing.

Based on the image resulting from the coherent signal processing, which was used for the hairiness measurement

* Corresponding author. Tel.: +351 253 510180.
E-mail addresses: vcarvalho@dei.uminho.pt (V. Carvalho), belsley@fisica.uminho.pt (M. Belsley), rosa@det.uminho.pt (R.M. Vasconcelos), fsoares@dei.uminho.pt (F.O. Soares).
[1] Tel.: +351 253 604320.
[2] Tel.: +351 253 510280.
[3] Tel.: +351 253 510180.

0263-2241/$ - see front matter © 2008 Elsevier Ltd. All rights reserved.
doi:10.1016/j.measurement.2008.02.010

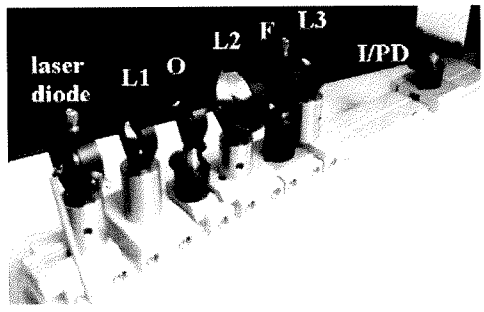

Fig. 1. Custom developed optical yarn measurement hardware.

Fig. 2. Example of an image resulting from coherent optical signal processing.

system (Fig. 1), it is possible to determine both the yarn hairiness and the diameter parameters. The hairiness corresponds to the total output voltage signal of all photodiodes in the linear array while the diameter corresponds to the number of photodiode elements (pixels) between the yarn contours. The contours of the yarn core are identified as the peak signals immediately adjacent to the 'valley' formed by the shadow of the yarn core.

2. Theoretical considerations

2.1. Line arrays

Linear arrays are photo detectors with multiple sensitive readable areas (pixels), organized over a single line [13]. These elements convert a spatial light distribution to a proportional current or voltage signal distributed sequentially in time. Some of the most important technical parameters of linear arrays are the total number of pixels, the pixel dimensions (width and height) (μm), the sensitivity (V/lx s), the wavelength range (nm), the dark signal (mV) and the saturation signal (V).

There are three different types of linear arrays, namely CCD (charged coupled devices), photodiodes and complementary metal-oxide semiconductor (CMOS), which have different production technologies and parameters. In our work, we selected a CMOS linear array. Similar to the CCD devices, this particular type of linear array uses metal-oxide semiconductor (MOS) structures, but the charge-to-voltage conversion occurs directly in the pixel cell, and not in the output, like the CCD. For this reason, CMOS technology arrays have generally somewhat more noise but also a higher sensitivity than CCD, as it is simpler to produce low power high gain amplifiers [13]. Fig. 4 presents the general structure of a CMOS linear array.

2.2. Line yarn characterization using a line array

If a line array with 512 pixels is placed orthogonally over the line profile reference in the image projection shown in Fig. 2, a signal similar to that presented in Fig. 5 would be obtained.

Fig. 5 represents the red plane intensity line profile signal which is proportional to the voltage signal resulting from the hairiness distribution image over the linear array photodiodes. It can be used for two purposes:

- Yarn hairiness spatial characterization – as it enables the determination of yarn hairiness spatial positions, which can be used, for example, to determine the position and projected length of the yarn fibres (Fig. 5) that protrude from the yarn core. Moreover, as the total signal is equivalent to the signal obtained from a single photodiode that covers the same area analysed by the linear profile, a full hairiness quantification statistical value is easily obtained for each yarn sample.
- Highly accurate yarn diameter characterization – which can be determined considering the number of pixels between the left and the right yarn contour pixels (Fig. 5)

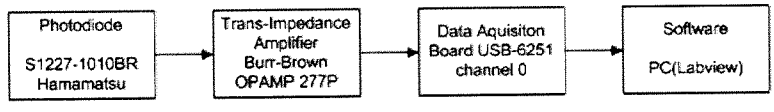

Fig. 3. Custom developed electronic yarn measurement hardware.

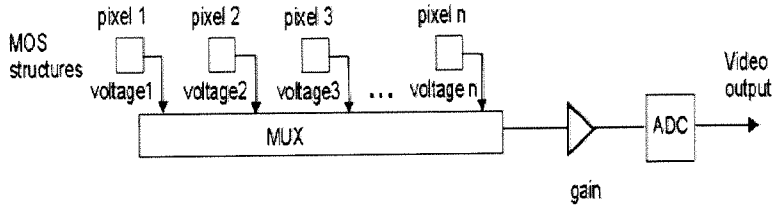

Fig. 4. General structure of a CMOS line array.

$$d = \frac{(\text{rycp} - \text{lycp})}{a}\text{pw} \times 1000 \quad (1)$$

where d is the yarn diameter (mm), rycp the right yarn contour pixel, lycp the left yarn contour pixel, a the optical amplification and pw is the pixel width (μm).

Despite the advantage of using a single device to characterize hairiness and diameter, the diameter measurement is the main feature of this system; it is due to the high precision achieved (each line array pixel has a width of few micrometers).

3. Developed work

3.1. Yarn diameter pixels determination using line profile image samples

After validating the system for quantifying yarn diameter, a simulation application was performed, using LabVIEW from NI [12], for characterizing the diameter of fifteen line profile samples similar to Fig. 5. Fig. 6 presents the red plane intensity diagrams of the considered samples.

An algorithm to determine the number of pixels between the yarn contours for each sample considered was developed. In this situation as the yarn core for all samples (Fig. 6) was located near the pixels interval centre, the following algorithm was used:

- *Step 1:* Determine the intensity average and substitute by zero, the pixels which have intensity values inferior to the average.
- *Step 2:* Use the intensity profile resulting from step 1, repeat the same procedure, for the pixels with nonzero intensity.
- *Step 3:* Determine a pixel index, starting in the pixel middle point index (256), placed between the yarn contours (pixel intensity equal to zero).
- *Step 4:* Start in the pixel index determined in step 3 and increase it pixel by pixel, to determine the pixel index corresponding to the first local maximum in the red plane intensity (right yarn contour pixel).

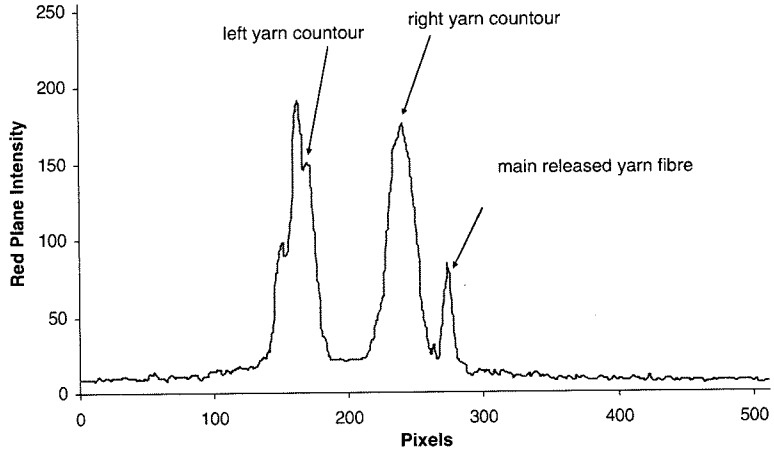

Fig. 5. Red plane line profile obtained for Fig. 2 with 512 pixels.

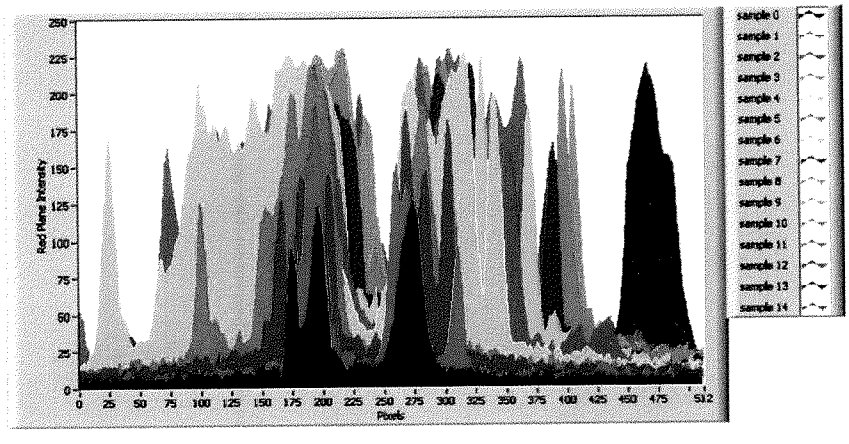

Fig. 6. Red plane intensity diagram of the considered 15 samples.

- *Step 5:* Start at the pixel index determined in step 3 and decrease it pixel by pixel, until reaching the first pixel index corresponding to a local maximum in the red plane intensity (left yarn contour pixel).
- *Step 6:* Determine the number of pixels between yarn contours (right yarn contour pixel – left yarn contour pixel), which corresponds to the yarn diameter in pixels.

The algorithm starts by identifying the pixels which register low intensity acquisition values (steps 1 and 2), in order to allow a clear identification of the yarn core. The yarn core position is characterized by low intensity values bracketed by pixels registering maximum intensity values (steps 4 and 5). Subsequently, a comparison with the overall pixels signal acquisition average is carried out recursively in the first two steps. In step 3, a pixel between the maximum intensity values identified in the previous two steps is obtained and registered as a low acquisition value. The reference pixel is defined for the tracking procedures of the yarn contours pixels described in steps 4 and 5. The yarn sample diameter, in pixels, corresponds to the number of pixels between the yarn contours (step 6).

Figs. 7–9 present the application of the described algorithm to sample 0.

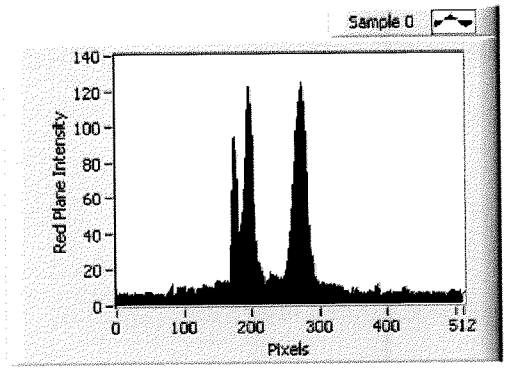

Fig. 7. Initial red plane intensity diagram for sample 0, which has average amplitude of 18.37.

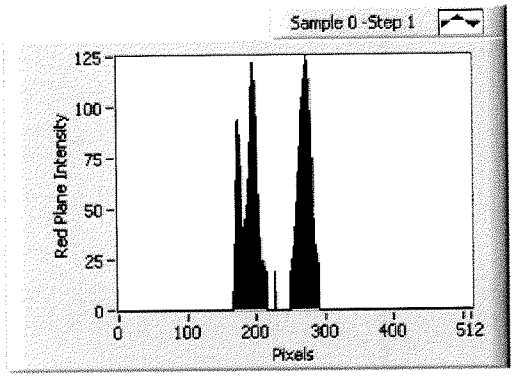

Fig. 8. Sample 0 after the application of Step 1, which has average amplitude of 64.24.

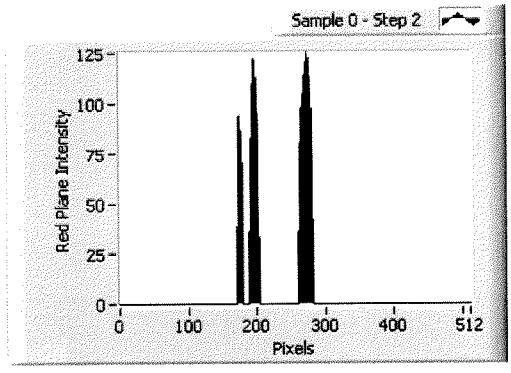

Fig. 9. Sample 0 after the application of Step 2.

After the application of step 2, we can observe that all the reduced amplitude pixel indexes were removed from the signal. Step 3 indicated that the centre pixel index (256) was placed between the yarn contours while steps 4 and 5 resulted in identifying pixels with indexes 196 and 275, corresponding to the red plane intensities amplitudes of 122 and 125, respectively, as the left and the right yarn contours. Finally, step 6 determined that the yarn diameter in the image plane is 79 pixels.

Table 1 presents the results of the algorithm for the analysed samples.

Considering the pixel diameter of each sample, we have determined the average (Fig. 10).

Fig. 10 displays the diameter ranging from 46 to 86 pixels, a variation range of 40 pixels with a standard deviation (SD) of 11.1 pixels. The average diameter measured was approximately 70 pixels. The corresponding percentage variation in the obtained diameters of each sample relative to the average is shown in Fig. 11.

The percent variation in diameter ranges between −35% and +22% with a SD of 15.7% for the samples studied. As the diameter variation is related to the mass variation, we can classify the type of irregularity [14–16] of each analysed sample as a thick place for positive variations inferior to 100% and as a thin place for negative variations. So, samples 0, 3, 4, 5, 6, 7, 10 and 12 are considered thick places and samples 1, 2, 8, 9, 11, 13 and 14 are considered as thin places. With the diameter variation results, all important diameter statistical results can also be determined.

3.2. Line array-experimental characterization

After the determination of yarn diameters based on the line profile analysis, we have developed an experimental setup based on the S8378-256Q CMOS line array and the C9001 Driver Circuit, both from Hamamatsu [17]. The main characteristics of the line array are

- 256 pixels.
- Pixel pitch of 25 μm.
- Pixel height of 0.5 mm.
- Maximum operating clock frequency of 500 kHz.
- Spectral response range from 200 to 1000 nm.

Table 1
Yarn diameter algorithm results obtained for each considered samples of Fig. 2

Sample	Initial amplitude average	Step 1 amplitude average	Initial yarn contours pixel	Left yarn contour pixel	Left yarn contour pixel amplitude	Right yarn contour pixel	Right yarn contour pixel amplitude	Pixels of diameter
0	18.34	64.24	256	196	122	275	125	79
1	28.10	97.15	253	195	190	260	152	65
2	38.10	110.12	256	205	144	268	187	63
3	53.83	138.49	256	199	200	283	189	84
4	98.82	181.48	256	184	223	270	208	86
5	82.55	157.22	256	203	203	274	200	71
6	59.99	120.64	256	203	205	276	218	73
7	70.41	152.96	256	220	182	294	213	74
8	72.91	159.21	256	216	227	281	223	65
9	79.96	159.07	256	235	185	281	224	46
10	96.10	171.48	256	215	211	297	224	82
11	60.76	111.36	256	231	199	293	141	62
12	59.12	126.60	256	218	198	300	220	82
13	70.77	142.11	256	231	149	292	184	61
14	33.08	68.78	256	234	100	297	149	63

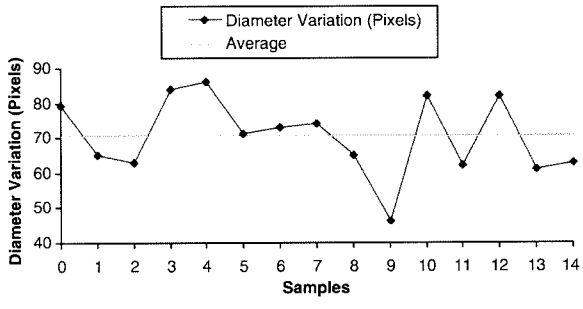

Fig. 10. Graphic representation of the variation in pixel diameter and the corresponding average obtained for the analysed 15 samples.

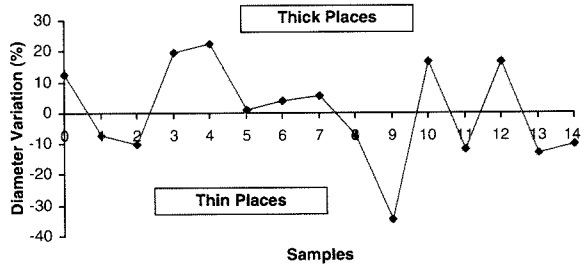

Fig. 11. Percentage diameter variation to average for the analysed 15 samples.

- Relative sensitivity between 80% and 100% for the used wavelength.
- Sensitivity of 4.4 V/lx s.
- On-chip charge amplifier.
- Built-in timing generator.
- Typical dark output voltage of 1.6 mV for low gain (used).
- Typical saturation output voltage of 2.5 V for low gain.
- Typical saturation exposure of 570 mlx s for low gain.
- Quartz window material.

The physical dimensions of the package are 15.8 mm width and 7.87 mm height; the active area has a width of 6.4 mm (256 pixels * 25 μm) and a height of 0.5 mm.

Fig. 12 presents the block diagram of the S8378-256Q CMOS linear array [17], where CLK corresponds to the pulse input to operate the shift register, ST starts the shift register operation, V_g is the external gain selector, V_{dd} is the supply voltage, V_{ss} is the ground, Video is the output signal and EOS is the end of the scan signal.

As Fig. 12 shows, the S8378-256Q is constituted by the 256 photodiodes, an address switch and a digital shift register to access the output data of each photodiode sequentially, a timing generator which enables the operation with only a start and clock pulse inputs, a selectable gain charge amplifier to convert the input charge of the capacitor to a voltage and a clamp circuit, which is used to prevent the output voltage of the charge amplifier to exceed a certain predetermined voltage level.

Associated to the line array, we have used the C9001 driver circuit. Its main features are

- Designed for all S8377/S3878 series CMOS line arrays.
- Operation with only two signals (start and clock) plus the +5 V supply.
- Output of a trigger signal.
- Offset output of 0.5 V.
- Saturation output from the offset between 3.3 and 4.0 V.

The driver circuit has a physical dimension of 50 × 12 mm and has integrated a sensor gain selection switch (low or high) which can be selected internally or externally.

Fig. 13 presents the connection interface of the C9001 driver circuit with the S8378-256Q and its block diagram [17].

As the C9001 interfaces with the line array sensor, the required timing chart is presented in Fig. 14 [17].

The clock (CLK) and start(START) signals are input signals, and the trigger (TRIG), end of conversion (EOS) and output (VIDEO) are output signals. The P-CLK, P-ST and GATE are internal signals for generating the clock, the start and the end of conversion signals, respectively.

As Fig. 13 shows, the clock signal is connected to the line array P-CLK directly from a buffer, the start signal is

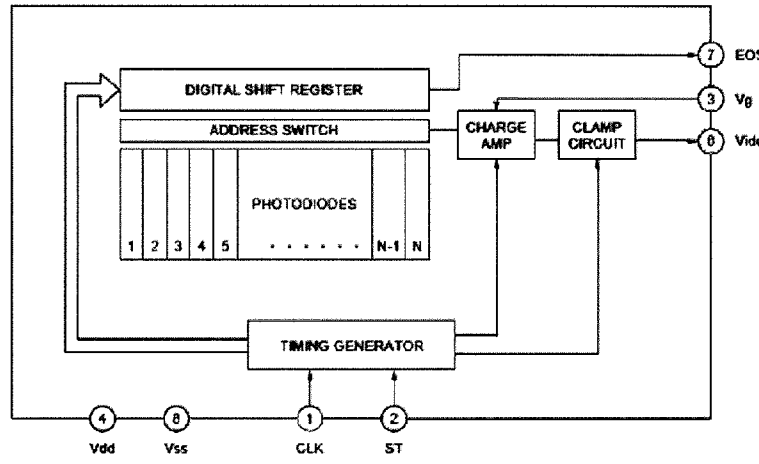

Fig. 12. Block diagram of the S8378-256Q CMOS line array.

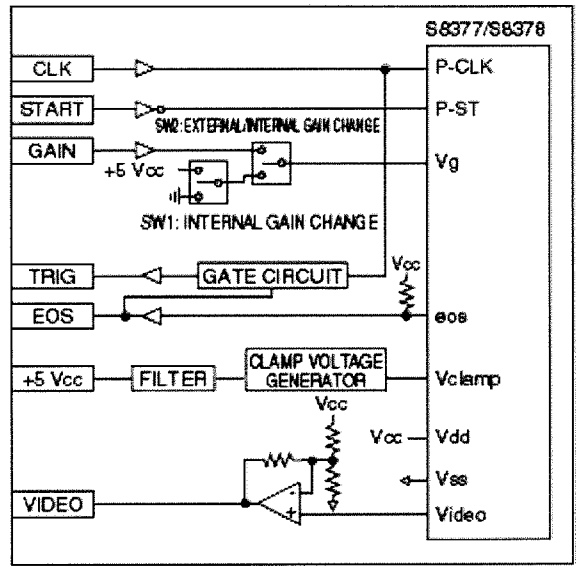

Fig. 13. Connection interface between the driver circuit and the S8378-256Q CMOS line array.

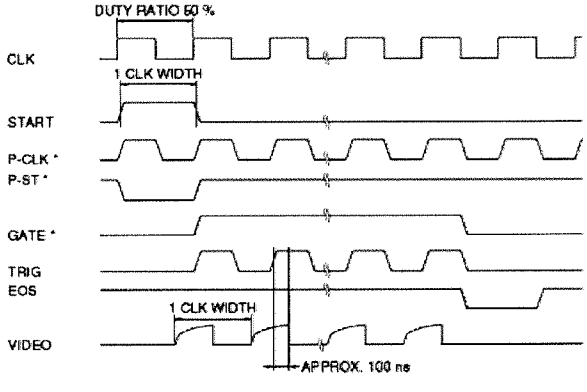

Fig. 14. Timing chart of the C9001 driver circuit.

inverted from a buffer, the trigger signal is created from the P-CLK signal plus an additional logical gate circuit and a buffer, while the end of conversion signal is created from the EOS signal plus a buffer and a logical gate circuit. The output video signal is connected to a non-inverted operational amplifier which enables one to obtain a higher output voltage using the driver circuit. Moreover, the $+V_{cc}$ signal interfaces with a stabilizing filter, which is connected to a voltage clamp generator to define its output limit.

We have used the USB6251 Data Acquisition Board from NI [12] to interface with the C9001 driver circuit. The clock and start signals were generated using counters 0 and 1 of the DAQ board which are available in outputs P2.4 and P2.5, respectively. The clock frequency is defined by the user in function of the yarn speed, with a pre-defined duty-cycle of 50%.

$$f_{clk} = \frac{y_{speed} \times 1000 \times (p_{number} + 1)}{l_{sample} \times 60} \tag{2}$$

where f_{clk} is the output clock frequency (Hz), y_{speed} the yarn velocity (m/min), p_{number} the line array number of pixels (256) and l_{sample} is the line array height (0.5 mm).

The start signal is generated automatically and is dependent of the clock frequency. The start frequency and the start duty-cycle are calculated

$$f_{start} = \frac{f_{clk}}{(p_{number} + 1)} \tag{3}$$

where f_{start} – output start frequency (Hz)

$$D_{start} = \frac{p_{number} + 1}{2 \times 50} \tag{4}$$

where D_{start} is the output start duty-cycle (%).

The output trigger signal of the C9001 driver circuit was connected to the PFI0 line of the DAQ board, which recognizes a logical positive transition, to determine the exact moment to begin signal acquisition. For the signal acquisition, we used channel 0 connected to the video signal of the driver circuit.

Fig. 15 presents the front panel of the developed virtual instrument used to manage and acquire the line array data.

An example containing the acquisition of four samples of the same section of yarn is presented in Fig. 16.

As the acquisition signal is continuous, a virtual instrument was developed to strip the signal sample by sample. So, the following stripping algorithm was used:

- *Step 1:* Identify the minimum voltage level, which happens between every yarn sample.
- *Step 2:* Identify the index samples where the minimum level is obtained.
- *Step 3:* Remove the acquisition signal, the samples with the indexes obtained in step 2.
- *Step 4:* Divide the signal obtained in step 3 in blocks of 256 samples where each block corresponds to a yarn sample.

Fig. 17 presents the application of the described algorithm to the samples shown in Fig. 16. As the samples were taken from the same position of the yarn, the stripping algorithm results in four completely overlapped profiles.

Regarding the diameter determination algorithm presented in Section 3, its application to experimental results requires an adaptation, because the shadow of the yarn core might not be close to the centre pixels of the linear array. The steps of the new version of the algorithm are

- *Step 1:* Subtract the voltage signal acquired without yarn from the acquisition signal.
- *Step 2:* Determine the average intensity and substitute by zero, the pixels which have intensity values inferior to the average.
- *Step 3:* Use the results of step 2, repeat the same procedure, for the remaining samples with nonzero intensity.

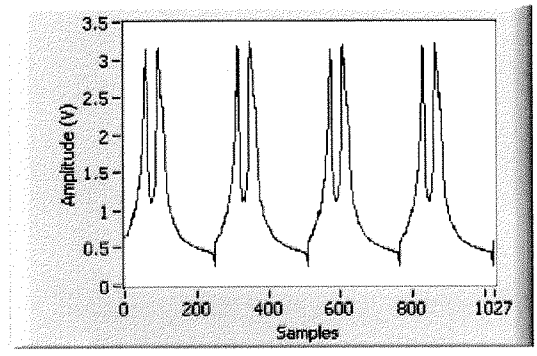

Fig. 16. Example of the signal resulting for the acquisition of four samples.

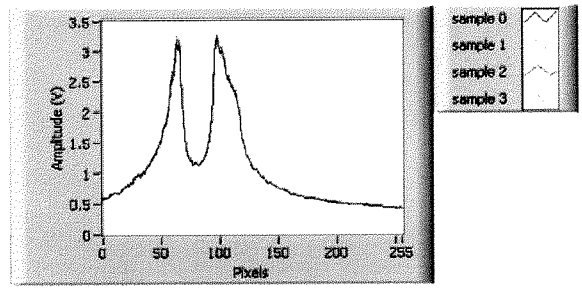

Fig. 17. Overlap signal resulting from the application of the striping sample algorithm.

- *Step 4:* Determine the index of the pixel corresponding to the maximum signal after step 3.
- *Step 5:* Determine, starting at index 0 and increasing, the first index which has a value superior to 0.

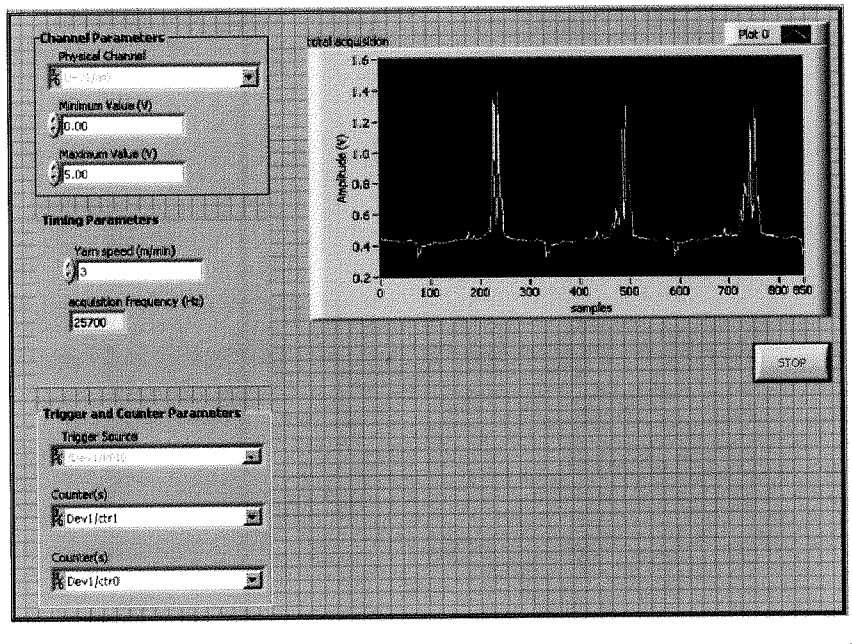

Fig. 15. Front panel of the developed virtual instrument for control and acquisition the signals from the CMOS line array.

- *Step 6:* Repeat the same procedure as in step 5 starting at index 255 and decreasing.
- *Step 7:* Calculate the absolute value of the difference between the index of the maximum pixel with the index determined in step 5.
- *Step 8:* Repeat the same procedure of step 8 but using the difference between the index of the maximum pixel with the index determined in step 6.
- *Step 9:* If the result of step 8 is superior to that of step 7, then the maximum index corresponds to the left yarn contour. If it is inferior, the maximum index corresponds to the right yarn contour.
- *Step 10:* If the maximum index is the left yarn contour, the right yarn contour is the index of the maximum amplitude value obtained between pixel index 255 and the first index equal to 0, counting from the left yarn contour index to the right. If the maximum index is the right yarn contour, the left yarn contour is the index of the maximum amplitude value obtained between pixel index 0 and the first index equal to 0, counting from the right yarn contour index to the left.
- *Step 11:* Determine the number of pixels between yarn contours (right yarn contour pixel – left yarn contour pixel), which correspond to the yarn diameter in pixels.

4. Experimental results

4.1. Sensibility

In order to determine the sensitivity of the developed experimental setup, the first test performed with the photodiode array considered a 295.00 g/km yarn, moved orthogonally in 10 steps of 0.1 mm, as presented in Fig. 18. A sample was acquired for each step.

Fig. 19 presents the signal acquisition of each step.

As the photodiode array has a height of 0.5 mm and each successive yarn sample is moved a distance of 0.1 mm, a fixed point of hairiness in the signal acquisition should be observed at most during five samples. So, if considering 10 samples, two certain fixed points could be observed. Fig. 19 presents the two selected fixed points observed between pixels 40 and 60 in the global signal acquisition (between 0 and 255 pixels). However, for a detailed analysis, Fig. 20 presents them between 47 and 55 pixels.

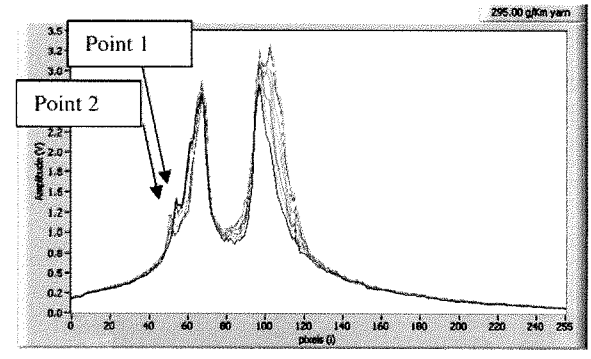

Fig. 19. Signal acquisition for each analysed yarn step.

As expected, each of the fixed points has five samples acquired sequentially. Moreover, it can be concluded from Fig. 20 that even such a small yarn step as 0.1 mm produces an identifiable signal change. The average signal also shows a measurable variation with the sample steps as shown in Fig. 21.

Fig. 21 shows a variation in the average signal amplitude over a range between 0.61 V and 0.72 V with a SD of 0.03 V.

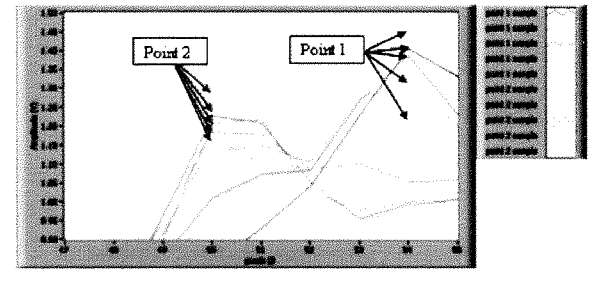

Fig. 20. Zoomed area between pixels 47 and 55.

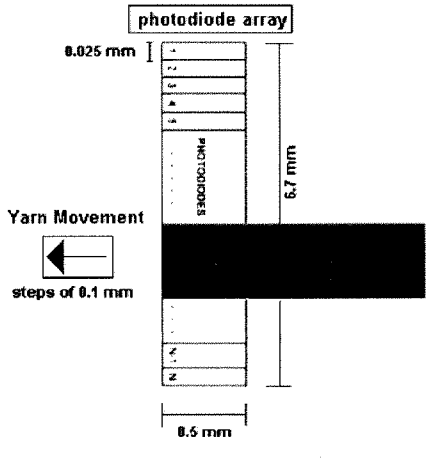

Fig. 18. Experimental setup configuration.

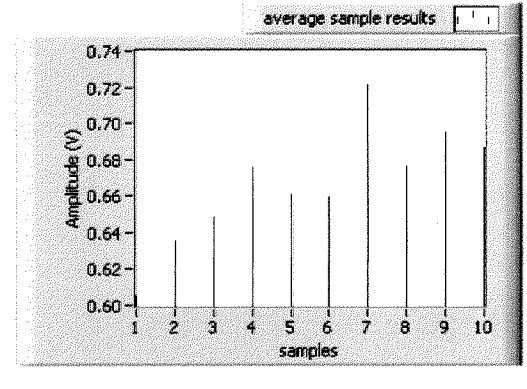

Fig. 21. Average amplitude obtained for each step sample.

4.2. Hairiness and diameter characterization for five different yarns

4.2.1. Sample acquisition

After verifying that good sensibility is obtained with the setup, five different types of cotton yarns were analysed. Table 2 presents the linear mass and the number of cables of each yarn.

For each yarn we have analysed 10 samples, in steps of 1 mm. Moreover, the light source gain was adjusted for each yarn, to allow a significant range of amplitude variation without saturation. Figs. 22–26 present the signal acquisition of each sample for each yarn, after removing the reference signal (signal without yarn – 0.37 V).

Table 2
Linear mass and number of cables of the tested yarns

Yarn linear mass (g/km)	Number of cables
19.67	1
36.88	1
49.17	2
62.00	1
295.00	3

4.2.2. Hairiness analysis

Afterwards, to study the hairiness variation, we have decided to focus on the limiting yarn cases. So, we have

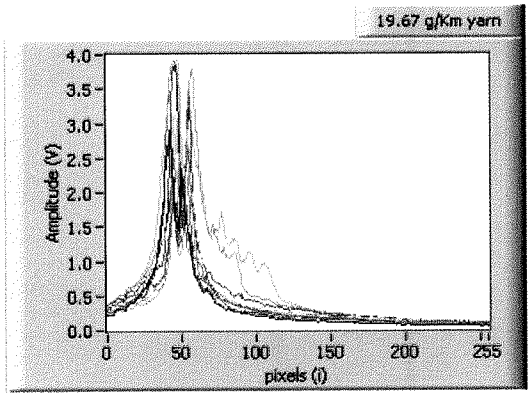

Fig. 22. Signal acquisition of the samples of the yarn with a linear mass of 19.67 g/km.

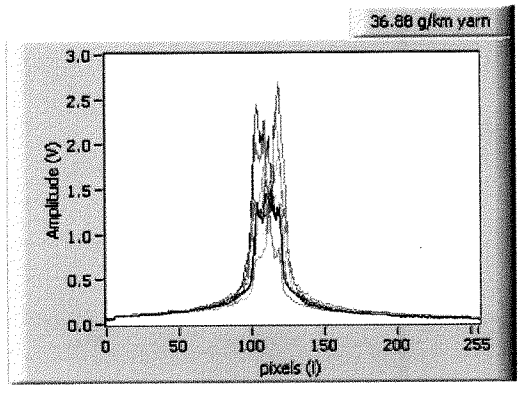

Fig. 23. Signal acquisition of samples of the yarn with a linear mass of 36.88 g/km.

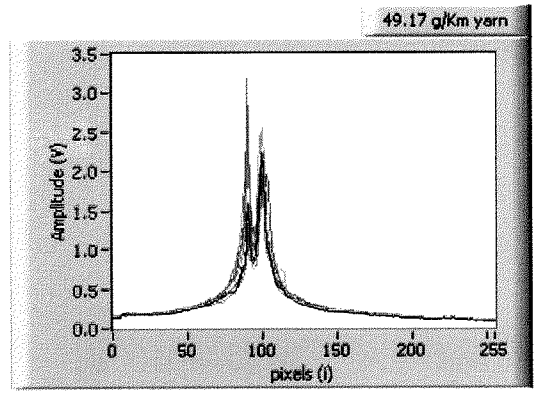

Fig. 24. Signal acquisition of the samples of the yarn with a linear mass of 49.17 g/km.

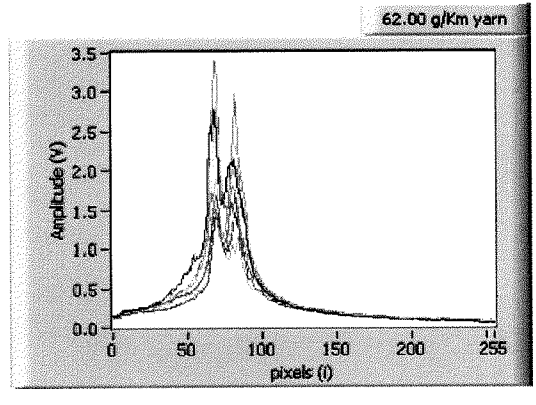

Fig. 25. Signal acquisition of the samples of the yarn with a linear mass of 62.00 g/km.

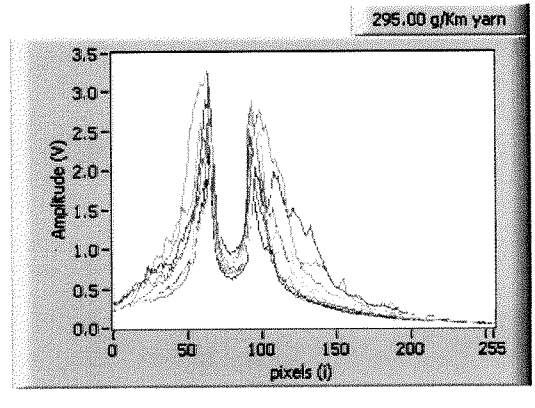

Fig. 26. Signal acquisition of the samples of the yarn with a linear mass of 295.00 g/km.

Table 3
SD result of each analysed sample for each yarn

Yarn (g/km)	Sample 1 SD	Sample 2 SD	Sample 3 SD	Sample 4 SD	Sample 5 SD	Sample 6 SD	Sample 7 SD	Sample 8 SD	Sample 9 SD	Sample 10 SD	Mean SD
19.67	0.54	0.43	0.38	0.43	0.55	0.42	0.53	0.69	0.89	0.92	0.58
36.88	0.31	0.50	0.47	0.27	0.31	0.28	0.32	0.47	0.42	0.39	0.37
49.17	0.32	0.31	**0.47**	0.39	0.41	**0.27**	0.37	0.33	0.35	0.36	**0.36**
62.00	0.58	0.45	0.36	0.37	0.56	0.65	0.37	0.30	0.27	0.36	0.43
295.00	0.58	0.71	0.70	0.63	0.54	**0.47**	0.51	0.46	**0.76**	0.70	**0.61**

determined the mean SD variation of the 10 samples in each yarn. Table 3 presents the obtained results.

Analysing Table 3, we can verify that the best case (yarn with a lower level of hairiness) is verified for the 49.17 g/km yarn and the worst case (yarn with a higher level of hairiness) is verified for the 295.00 g/km yarn. These results agree completely with Figs. 28 and 30 which are, respectively, the graphical results which present lower and higher variations.

Using these results, a closer observation was performed for samples 3 and 6 of the 49.17 g/km yarn (Figs. 27 and 28) and for samples 9 and 6 of the 295.00 g/km yarn (Figs. 29 and 30), which correspond, respectively, to the samples with highest and lowest SD results.

Comparing the samples with higher SD values (samples 3 and 9 of the 49.17 and 295.00 g/km yarns, respectively) with the samples with lower values of SD (samples 6 of the 49.17 and 295.00 g/km yarns, respectively), as expected, a higher range of amplitude deviation is obtained for the samples with higher SD. In terms of hairiness geometry, no released yarn fibres could be observed on these samples because no spikes are observed from the right and left yarn contours. Some examples of samples with released yarn fibres, indicated with arrows, can be observed in samples 10 of 19.67 g/km yarn, 3 and 7 of 295.00 g/km yarn, as presented in Figs. 31–33, respectively.

Analysing Figs. 31–33, it is verified that all samples have released fibres from the right yarn contour but only samples 7 and 3 of the 295.00 g/km yarn also verified a released fibres in the left yarn contour side. Moreover, when considering the hairiness variation (%) from the average, the signal generated from the yarn released fibres has

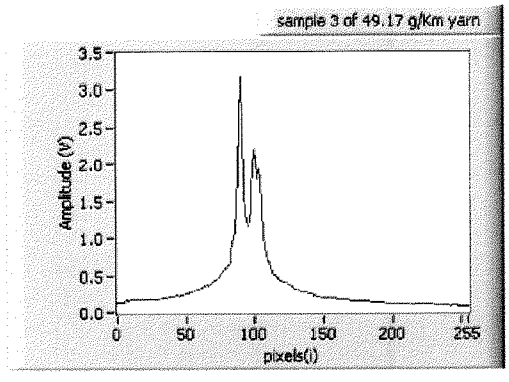

Fig. 27. Signal acquisition of sample 3 of the 49.17 g/km yarn.

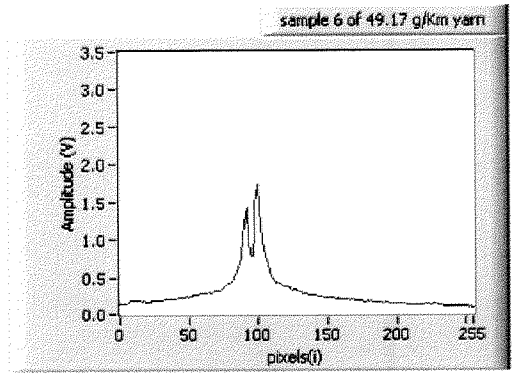

Fig. 28. Signal acquisition of sample 6 of the 49.17 g/km yarn.

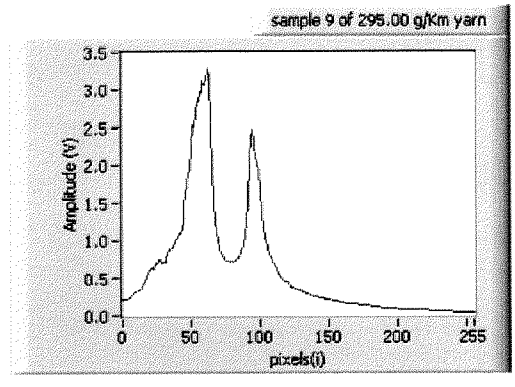

Fig. 29. Signal acquisition of sample 9 of the 295.00 g/km yarn.

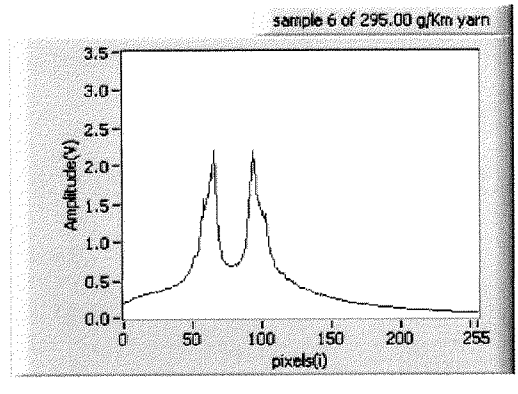

Fig. 30. Signal acquisition of sample 6 of the 295.00 g/km.

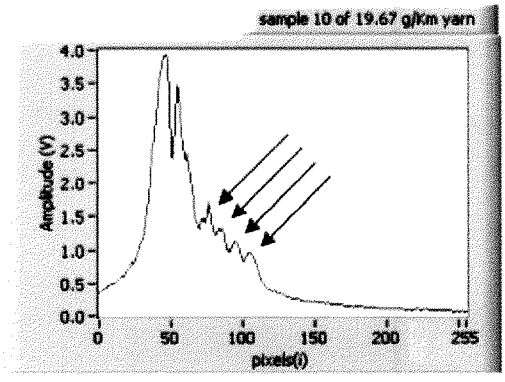

Fig. 31. Signal acquisition of sample 10 of the 19.67 g/km yarn.

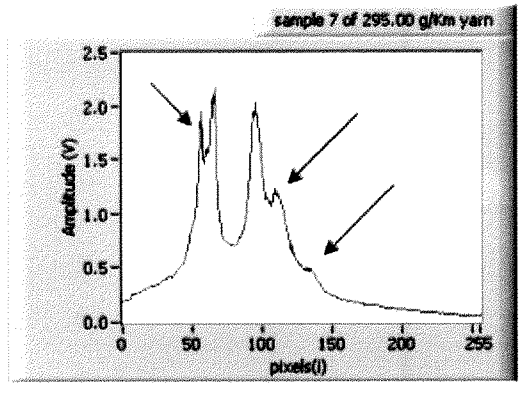

Fig. 32. Signal acquisition of sample 7 of the 295.00 g/km yarn.

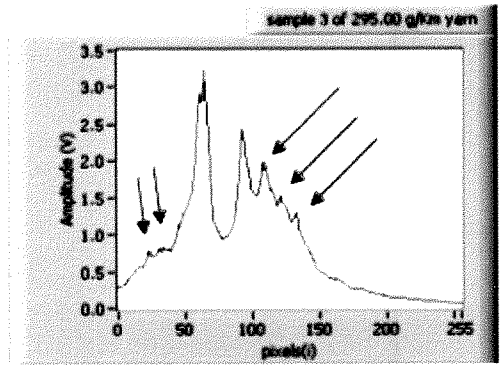

Fig. 33. Signal acquisition of sample 3 of the 295.00 g/km. yarn

the higher "weight", because the contours signal is characterized, generally, by a similar signal, operating like a DC component. Table 4 presents the average results obtained for each sample and the mean value of yarns 49.17 g/km and 295.00 g/km, respectively.

Then, using the results of Table 4, the signal variation, which is proportional to the hairiness variation from the average, was determined (Fig. 34).

$$H_{(\%)} = \frac{x_i - \bar{x}}{\bar{x}} 100 \quad (5)$$

where H is the hairiness variation from the average (%), x_i the sample (V) and $\bar{x}$ is the average (V).

Analysing Fig. 34, we can verify that in agreement with the mean SD results (Table 3), the 295.00 g/km yarn has a larger range of variation [−26.67; 33.33] (%) against [−12.50; 12.50] (%) of the 49.17 g/km yarn. This leads to a SD variation result of 7.51% and 18.92% for yarns 49.17 and 295.00 g/km, respectively. The superior limits are obtained for samples 3 of both yarns (underlined bold results shown in Table 4) and the inferior limits for samples 6 and 8 (bold results shown in Table 4), of yarns 49.17 and 295.00 g/km, respectively. Figs. 35–39 represent the acquisition signals for these samples.

As expected, the samples corresponding to the superior limits (Figs. 35 and 37) have higher signal amplitudes than the inferior limit samples (Figs. 36 and 38).

Finally, considering the variation results shown in Fig. 38, it is possible to determine all relevant hairiness parameters, as previously done with a single photodiode [1–6].

4.2.3. Diameter analysis

Fig. 39 presents the diameter, in number of pixels, obtained for each different yarn over ten samples. This measurement was performed using the yarn diameter determination algorithm described in Section 3.2.

In Fig. 39, it is observed that the 295.00 g/km has the higher diameter, followed by the 62.00 g/km yarn. However, for the other yarns, the diameter distinction is not so clear with this reduced number of samples. The mean and SD values for each yarn are presented in Table 5.

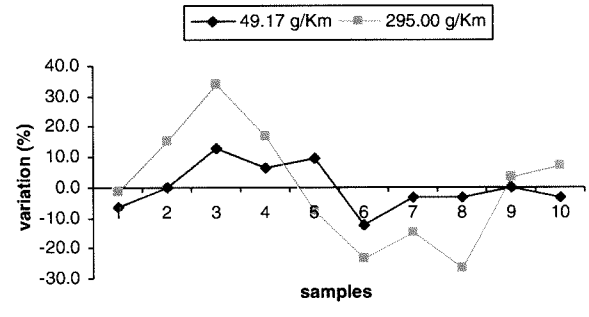

Fig. 34. Percentage signal variation to average of the samples of yarns 49.17 and 295.00 g/km.

Table 4
Average results of each analysed sample for yarns with linear masses of 49.17 and 295.00 g/km

Yarn (g/km)	Sample 1 AV	Sample 2 AV	Sample 3 AV	Sample 4 AV	Sample 5 AV	Sample 6 AV	Sample 7 AV	Sample 8 AV	Sample 9 AV	Sample 10 AV	Mean AV
49.17	0.30	0.32	**0.36**	0.34	0.35	**0.28**	0.31	0.31	0.32	0.31	0.32
295.00	0.59	0.69	**0.80**	0.70	0.55	0.46	0.51	**0.44**	0.62	0.64	0.60

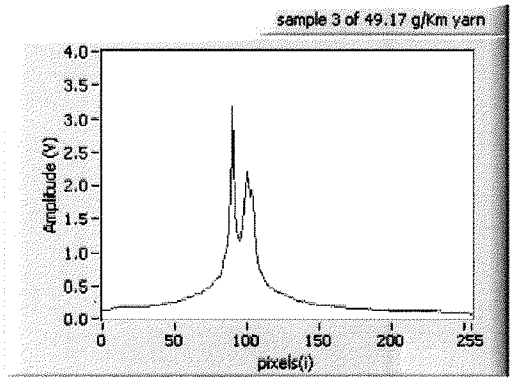

Fig. 35. Signal acquisition of the sample 3 of 49.17 g/km yarn.

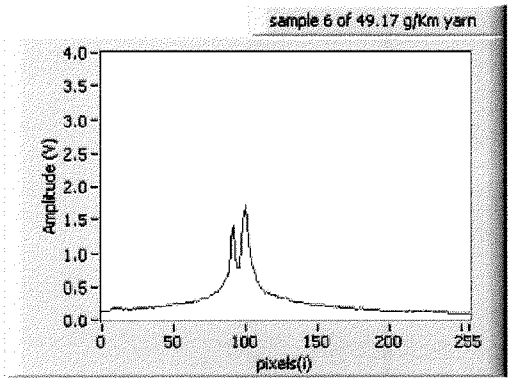

Fig. 36. Signal acquisition of the sample 6 of 49.17 g/km yarn.

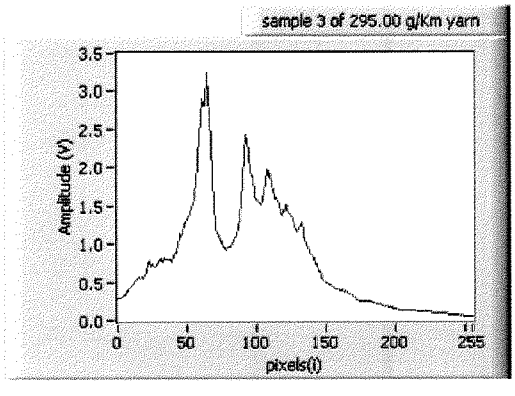

Fig. 37. Signal acquisition of the sample 3 of 295.00 g/km yarn.

Using the average results obtained in Table 5, the 62.00 g/km yarn is followed by the 49.17 g/km. Still, if considering only the average results, as the 19.67 and 36.88 g/km yarns present a similar value (8.10), and it is not possible to distinguish them. Nevertheless, when considering SD it becomes clear that the thinner yarn is the 19.67 g/km because it has a lower SD value (1.73), being a more regular yarn. This claim is supported by the fact that high linear masses have, generally, an increased probability of

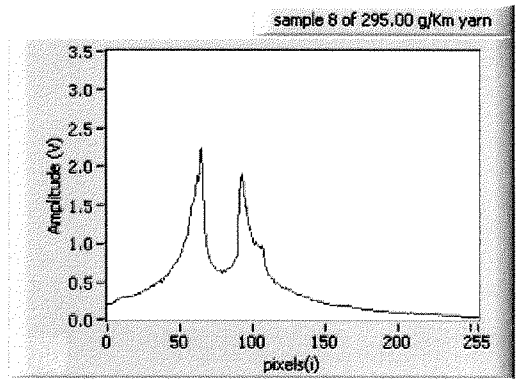

Fig. 38. Signal acquisition of the sample 8 of 295.00 g/km yarn.

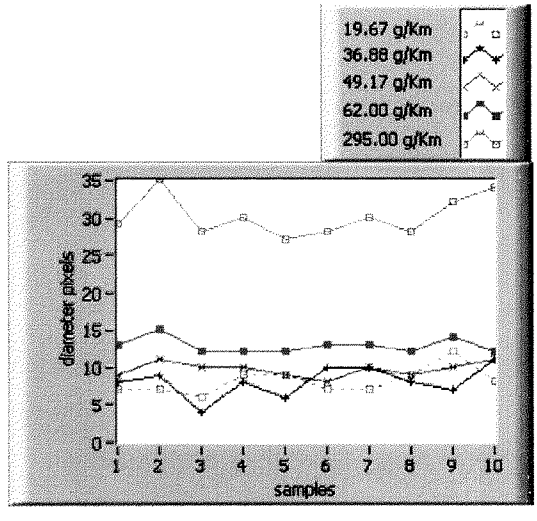

Fig. 39. Number of diameter pixels obtained for each sample in all tested yarns.

Table 5
Diameter pixels average and SD results obtained for all tested yarns

Yarn linear mass (g/km)	Diameter pixels average	Diameter pixels SD
19.67	8.10	1.73
36.88	8.10	2.08
49.17	9.70	0.95
62.00	12.80	1.03
295.00	30.10	2.73

being characterized by superior values of diameter SD, as could be verified by the 295.00 which has the maximum value. So, as expected, there is a direct relationship between the yarn linear mass and the yarn diameter, higher the linear mass, the larger the diameter.

Similar to the hairiness analysis, we will consider only the limiting yarn cases (19.67 and 295 g/km). Table 6 presents some of the step results of the diameter determination algorithm for the maximum and minimum diameter samples.

Analysing Table 6, for the thinner yarn (19.67 g/km), the minimum diameter (6 pixels) is obtained for the sample

Table 6
Step results of the diameter determination algorithm for the limit diameter samples in yarns 19.67 and 295 g/km

Yarn linear mass (g/km)	Sample index	Step 2 AV	Step 3 AV	Step 4 AV	Step 5 max index	Step 6 first index	Step 7 first index	Step 8 ABS	Step 9 ABS	Step 10 max side contour	Step 11 max index other side contour	Step 12 number of diameter pixels
19.67	3	0.34	0.78	1.34	51	42	54	9	3	Right	45	6
	9	0.68	1.83	2.96	45	41	58	4	13	Left	57	12
295.00	5	0.55	1.12	1.69	93	64	99	29	6	Right	66	27
	2	0.69	1.48	2.20	98	61	105	37	7	Right	63	35

index 3 (non-bold index) and the maximum diameter (12 pixels) is obtained for the sample index 9 (bold index). This yarn presents a variation of 100% in diameter. For the thicker yarn (295.00 g/km) the minimum diameter (27 pixels) is obtained for the sample index 5 (non-bold index) and the maximum diameter (35 pixels) is obtained for the sample index 2 (bold index). This yarn presents a variation of 22.9% of diameter. Figs. 40–43 present the acquisition signals of the samples considered.

In Figs. 40 and 41, the left and right contour pixels are indicated by arrows. In Fig. 40 (minimum diameter of yarn 19.67 g/km), the left contour index is obtained for pixel 45 and the right contour index is obtained for pixel 51, resulting as determined by the algorithm in a diameter of 6 pixels. In Fig. 41 (maximum diameter of yarn 19.67 g/km), the left contour index is obtained for pixel 45 and the right contour index is obtained for pixel 57, achieving a diameter of 12 pixels as determined by the algorithm.

In Figs. 42 and 43, we present the acquisition signals for samples 2 and 5 of the 295.00 g/km yarn. The left and right contour pixels are indicated by arrows. In Fig. 42 (minimum diameter of yarn 295.00 g/km), the left contour index is obtained for pixel 66 and the right contour index, for pixel 93, resulting in a diameter of 27 pixels. In Fig. 43 (maximum diameter of yarn 295.00 g/km) the left contour index is obtained for pixel 63 and the right contour index is obtained for pixel 98, resulting in a diameter of 35 pixels.

As stated before, to determine the yarn diameter in the image plane from the number of pixels it is necessary to

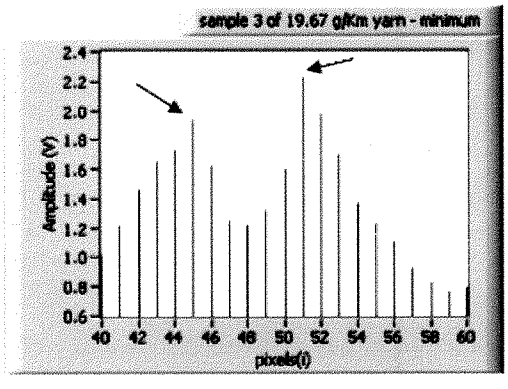

Fig. 40. Signal acquisition of sample 3 for the 19.67 g/km yarn.

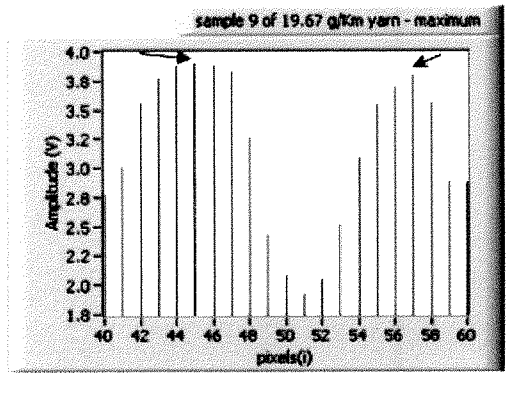

Fig. 41. Signal acquisition of sample 9 for the19.67 g/km yarn.

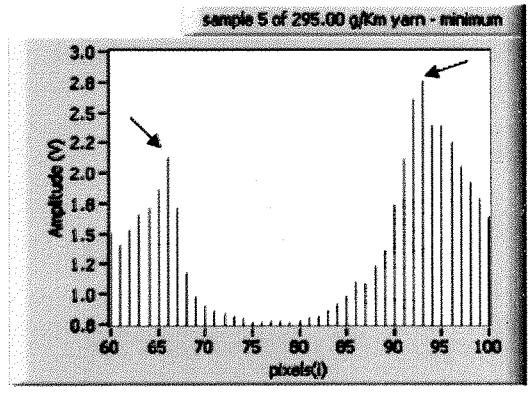

Fig. 42. Signal acquisition of sample 5 for the 295.00 g/km yarn.

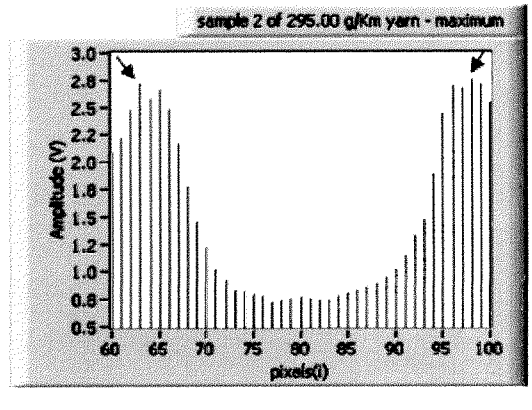

Fig. 43. Signal acquisition of sample 2 for the 295.00 g/km yarn.

multiply the number of pixels by the pixel pitch, which in this case is 25 μm. Fig. 44 presents the image plane diameter for each sample of the 19.67 and 295 g/km yarns.

As the optical configuration used has an amplification factor of approximately 0.7 (reduction), the object plane diameter (real dimension) is obtained dividing the image plane results by the amplification factor. Fig. 45 presents the object plane diameter in each sample of the 19.67 and 295 g/km yarns.

Table 7 presents the object plane diameter results obtained for the maximum and minimum diameters of each yarn.

From Table 7, it is verified that in the object plane, yarn 19.67 g/km varies between 214.3 μm and 428.6 μm and yarn 295.00 g/km varies between 964.3 μm and 1250 μm, with an error which varies between 2.9% and 16.7%, considering that the minimum error should be 1 pixel. In order to validate the determined diameters, we have compared the values to those measured using images acquired with an electron microscope, as presented in Figs. 46 and 47. Fig. 46 presents an electron microscope picture of the 295.00 g/km yarn.

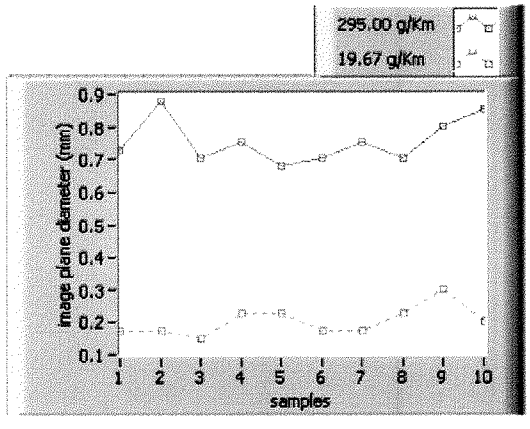

Fig. 44. Image plane diameter variation for each sample of yarns 19.67 and 295.00 g/km.

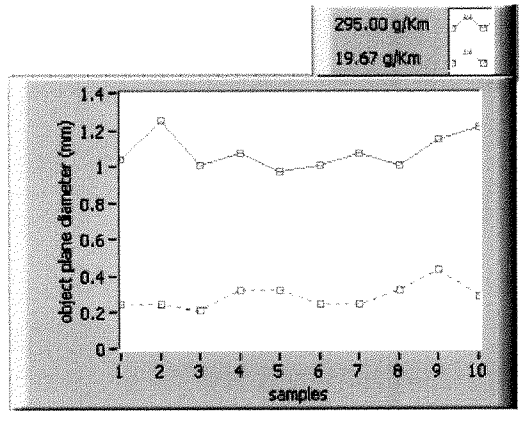

Fig. 45. Object plane diameter variation for each sample of yarns 19.67 and 295.00 g/km.

Table 7
Limit object plane diameter results of the samples in yarns 19.67 and 295 g/km

Yarn linear mass (g/km)	Sample index	Image plane diameter (μm) (number of diameter pixels × 25 μm)	Object plane diameter (number of diameter pixels × 25 μm)/0.7
19.67	3 Minimum	150	214.3 μm ±16.7%
	9 Maximum	300	428.6 μm ±8.3%
295.00	5 Minimum	675	964.3 μm ±3.7%
	2 Maximum	875	1250 μm ±2.9%

The yarn from Fig. 46 (295.00 g/km) has diameter variations from 0.99 mm to 1.22 mm, measured with the electron microscope, which are ranges that agree perfectly with the object plane diameters as presented in Table 7.

Fig. 47 presents an electron microscope picture of the 19.67 g/km yarn.

The yarn from Fig. 47 has a diameter that varies from 0.29 mm to 0.44 mm, as measured in the image acquired with the electron microscope. This range, as was the case for the thicker yarn (Fig. 46), is within the values quoted in Table 7. The lower limit in the electron microscope image is in fact somewhat thicker than the minimum

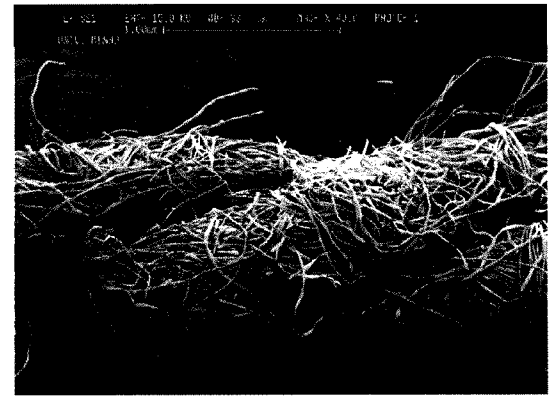

Fig. 46. Electron microscope picture of the 295.00 g/km yarn.

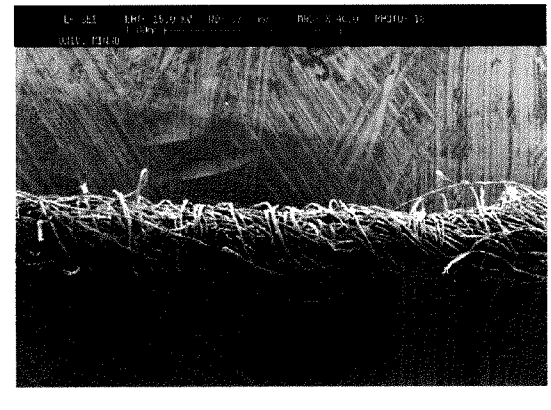

Fig. 47. Electron microscope picture of the 19.67 g/km yarn.

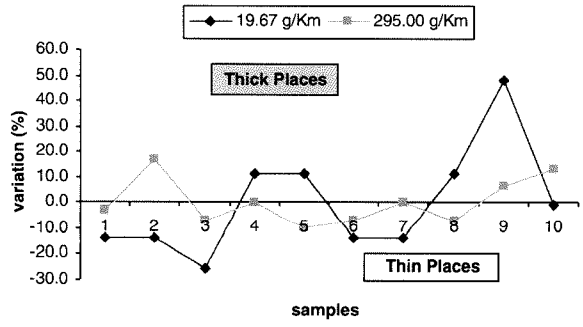

Fig. 48. Percentage signal variation to average of the object plane diameter samples of yarns 19.67 and 295.00 g/km.

diameter found using the linear photodiode array (290 μm compared to between 178 μm and 250 μm). But this yarn is a single cable non-re-torsion yarn, and so without a clear diameter variation pattern, higher diameter variations could easily occur. We have no reason to rule out larger variations than those observed in the electron microscope image; it maybe that sample 3 corresponds to a particularly thin point in the yarn.

Afterwards, considering the object plane diameters presented in Fig. 44, we have determined their variations compared to the mean values, as presented in Fig. 48.

The percentage variation in diameter ranges between −25.93% and +48.15%, for the 19.67 g/km yarn, which leads to a SD of 21.3%. For the 295.00 g/km yarn, a percentage diameter range variation between −10.30% and +16.28% is obtained, which leads to a SD of 9.1%. As stated before, the diameter variation is related to the linear mass variations, which enable the classification of the type of irregularity of each analysed sample as a thick place for positive variations inferior to 100% and as a thin place for negative variations. So, for the 19.67 g/km yarn, samples 4, 5, 8 and 9 are considered thick places and samples 1, 2, 3, 6, 7 and 10 are considered thin places. Similarly, for the 295 g/km yarn, samples 2, 9 and 10 are considered thick places and samples 1, 3, 5, 6 and 8 are considered thin places; samples 4 and 7 do not present variations relative to the mean value and so have no irregularities.

Comparing the variation results of both yarns, the 295.00 g/km is considered more regular than the 19.67 g/km yarn, as it presents diameter variations within a short range, as can be quantified by the lower SD result.

5. Conclusions and future work

The presented yarn characterization approach using a system based on a photodiode array presents the following advantages:

- Possibility of measuring hairiness, irregularities and diameter using one optoelectronic device.
- High level of diameter measurement precision, as the optoelectronic device used has a pitch of 25 μm and so could be considered as microscopically precise. This accuracy can in fact be improved by altering the amplification factor of the optical system or even by using a photodiode array with a smaller pitch.
- Possibility of the precise characterization of irregularities based on diameter variations with very high sensitivities.
- Spatial characterization of the prominent fibres released from the yarn core (hairiness) by identifying the pixels corresponding to the signal provoked by these fibres.
- Optical setup optimization.
- System portability (reduced weight and volume).

Nevertheless, the system has the following drawbacks:

- High final cost, considering the required acquisition hardware (photodiode array + driver) and the data processing unit (requires a fast computer with a considerable amount of disc space and memory).
- Complex operation, as the photodiode array requires accurate timing circuits.
- High computational effort, considering the data processing from the high number of samples (257 in this case) for each yarn sample (ex: for a 12 m/min yarn speed the sample rate it is approximately 103 kHz).
- Requirement of an optical setup with an inferior amplification factor, considering that the yarn image including hairiness should have a maximum width of 6.4 mm (width of the photodiode array).

For commercial purposes, the use of the photodiode array based system is oversized. A simpler solution considering two orthogonal photodiodes based system might be sufficient and less expensive for the common yarn characterization. This alternative is justified by the fact that irregularities are normally defined commercially, for variations starting at ±30%, which is a level of variation that might be correctly measured by a single photodiode for the majority of yarns parameters. However, the superior precision of the photodiode array based apparatus may be employed to accurately characterize the diameter variations of the small sections of yarn or to perform innovative studies concerning the spatial positions of the fibres associated with yarn hairiness.

Acknowledgement

The authors are grateful to the Portuguese Foundation (FCT) for funding through the scholarship (BD/19028/2004).

References

[1] V. Carvalho, P. Cardoso, M. Belsley, R. Vasconcelos, F. Soares, Determination of yarn hairiness using optical sensors, in: EUROSENSORS XX, Gothenburg, Sweden, 2006.
[2] V. Carvalho, P. Cardoso, M. Belsley, R. Vasconcelos, F. Soares, Development of a yarn evenness measurement and hairiness analysis system, in: IECON06, Paris, France, 2006.
[3] V. Carvalho, P. Cardoso, M. Belsley, R. Vasconcelos, F. Soares, Yarn hairiness parameterization using a coherent signal processing technique, Sensors and Actuators 142 (1) (2008) 217–224.
[4] V. Carvalho, P. Cardoso, M. Belsley, R. Vasconcelos, F. Soares, A new statistical reference method for yarn hairiness quantification, ISIE 2007, 4–7 June, Vigo, Spain, pp. 1864–1869.
[5] V. Carvalho, P. Cardoso, M. Belsley, R. Vasconcelos, F. Soares, Optical yarn hairiness measurement system, INDIN07, 23–27 July 2007, Vienna, Austria, vol. I, pp. 359–364.

[6] V. Carvalho, P. Cardoso, M. Belsley, R. Vasconcelos, F. Soares, Yarn diameter measurement using coherent optical signal processing, IEEE Sensors Journal, in press.
[7] J.W. Goodman, Introduction to Fourier Optics, McGraw-Hill, Greenwood Village, 1996.
[8] E.G. Steward, Fourier Optics: An Introduction, Dover Publications, New York, 2004.
[9] P.M. Duffieux, The Fourier Transform and its Applications to Optics, second ed., John Wiley & Sons, New York, 1983.
[10] C.K. Madsen, Optical Filter Design and Analysis: A Signal Processing Approach, Wiley-Interscience, New York, 1999.
[11] S. Franco, Design with Operational Amplifiers and Analog Integrated Circuits, third ed., Mc-Graw Hill, Greenwood Village, 2001.
[12] <www.ni.com>.
[13] JETI Technische Instrumente GmbH, Basics of Spectral Measurement, JETI, Jena, 2005.
[14] V. Carvalho, Parametrização de Fio Têxtil Baseada na Análise de Massa., M.Sc. Thesis, Minho University, Guimarães, Portugal, 2002.
[15] R. Furter, Evenness Testing in Yarn Production: Part I, The Textile Institute and Zellweger Uster AG, Manchester, 1982.
[16] J.S. Neves, A Irregularidade dos Fios Têxteis, sua origem, medição e análise, Oporto, 1968.
[17] <www.hamamatsu.co.jp>.